



Anomalous Diffraction in Cold Magnetized Plasma

Z. Abelson,^{1,*} R. Gad,² S. Bar-Ad,¹ and A. Fisher²

¹*Sackler School of Physics and Astronomy, Faculty of Exact Sciences, Tel-Aviv University, Tel Aviv 6997801, Israel*

²*Department of Physics, Technion-Israel Institute of Technology, Haifa 3200003, Israel*

(Received 29 September 2014; revised manuscript received 29 July 2015; published 28 September 2015)

Cold magnetized plasma possesses an anisotropic permittivity tensor with a unique dispersion relation that for adequate electron density and magnetic field results in anomalous diffraction of a right-hand circularly polarized beam. In this work, we demonstrate experimentally anomalous diffraction of a microwave beam in plasma. Additionally, decreasing the electron density enables observation of the transition of the material from a hyperbolic to a standard material. Manipulation of the control parameters will enable plasma to serve as a reconfigurable metamaterial-like medium.

DOI: 10.1103/PhysRevLett.115.143901

PACS numbers: 42.25.Bs, 52.40.Db, 52.35.Hr

The control of wave propagation in hyperbolic metamaterials has been widely demonstrated in a variety of systems and has aroused much interest in recent years [1]. This distinct class of metamaterials, defined as possessing mixed positive and negative principal elements in either their permittivity or permeability tensors, has displayed focusing effects [2], subwavelength imaging [3], and even an enhancement of spontaneous emission [4]. Zhang *et al.* [5] have proposed cold magnetized plasma as such a medium that shall demonstrate almost diffractionless propagation of the electromagnetic waves in the direction of the magnetic field, the reason being that magnetized plasma possesses an anisotropic permittivity tensor leading to a unique dispersion relation that, under the correct conditions, will induce an anomalous diffraction of right-hand circularly polarized (RHCP) electromagnetic waves below the cyclotron frequency. Anomalous diffraction corresponds to an opposite sign to that occurring in nature. Experimentally, early work by Fisher *et al.* has demonstrated resonance cones in a magnetized plasma [6]. However, the investigation of resonance cones has been limited to dipolar radiation, while beam propagation has not been examined. Fresh interest has been generated in regard to such optical phenomena in plasma by the work of Gad *et al.* [7], demonstrating a newly predicted optical effect in plasma, magnetically induced transparency, a classical analogue to the quantum effect of electromagnetically induced transparency.

This work demonstrates an additional, previously unobserved optical effect in plasma, anomalous propagation of electromagnetic radiation in a cold magnetized plasma. Additionally, due to the dynamic nature of the plasma in our system, we are able to examine the transition of the plasma from a hyperbolic to a standard material. First, the theoretical basis for the occurrence of the anomalous diffraction effect is briefly reviewed. Next, the experimental system and plasma diagnostics are presented. Finally, experimental results providing evidence of the effect and

simulations replicating the results are presented and discussed.

As a simplification, we consider the propagation of electromagnetic waves in an infinite Lorentz plasma of uniform density. In this model the electrons are described as a charged fluid in a stationary positive background representing the ions. Effects of electron temperature have been neglected due to the assumption that the temperature is sufficiently low. For an infinite cold plasma in an external magnetic field $B_0\hat{z}$, with a plasma particle density n_e of uniform distribution, the relative permittivity tensor is given by [8]

$$\epsilon_r = \begin{pmatrix} \epsilon_1 & -i\epsilon_2 & 0 \\ +i\epsilon_2 & \epsilon_1 & 0 \\ 0 & 0 & \epsilon_p \end{pmatrix}, \quad (1)$$

where $\epsilon_1 \equiv 1 - (\omega_p^2/\omega^2)[(\omega^2)/(\omega^2 - \omega_c^2)]$, $\epsilon_2 \equiv (\omega_p^2/\omega^2) \times [(\omega_c\omega)/(\omega^2 - \omega_c^2)]$, and $\epsilon_p \equiv 1 - (\omega_p^2/\omega^2)$. ω is the angular frequency of the propagating electromagnetic wave, ω_c is the cyclotron frequency, and ω_p is the plasma frequency.

Recently, Pendry has shown that a negative permittivity holds a significant effect on the electromagnetic properties of a material, noting especially an effect of strong focusing [9,10]. Furthermore, it has been determined that anisotropic media possessing opposite signs of diagonal permittivity tensor elements exhibit a unique dispersion relation leading to novel phenomena, including negative refraction, near-field focusing, and high impedance surface reflection [11]. Considering plasma, the permittivity tensor can exhibit elements of mixed signs as a function of the magnitude of the magnetic field and the electron density.

The dispersion relation of magnetized plasma is given by the Appleton equation [12]:

$$\tan^2\theta = -\frac{\epsilon_p[\mu^2 - (\epsilon_1 + \epsilon_2)][\mu^2 - (\epsilon_1 - \epsilon_2)]}{(\mu^2 - \epsilon_p)[\epsilon_1\mu^2 - (\epsilon_1^2 - \epsilon_2^2)]}, \quad (2)$$

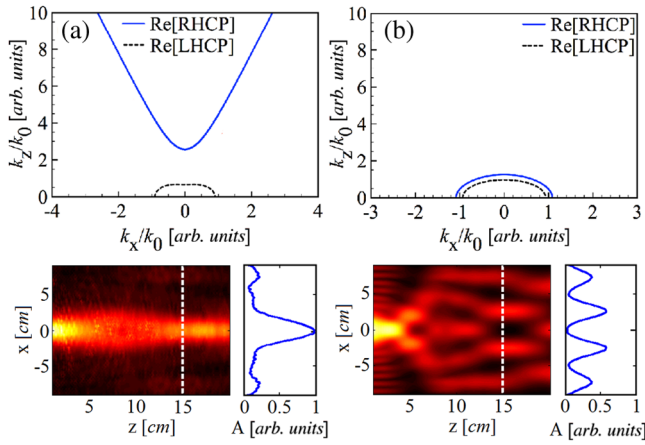


FIG. 1 (color online). Top: Comparison between EFCs for different electron densities. These EFCs were calculated for a frequency of 7.9 GHz, an external magnetic field of 0.35 T, and an electron density of (a) $1 \times 10^{12} \text{ cm}^{-3}$ and (b) $1 \times 10^{11} \text{ cm}^{-3}$. (a) A hyperbolic EFC. Note that for (b) the EFC is similar to the EFC in vacuum, allowing propagation at all angles. In this case, the plasma will not exhibit anomalous diffraction. Bottom: Poynting vector amplitude obtained by numerical COMSOL simulations of a RHCP beam propagating from a slit for plasmas with the same densities as in (a) and (b). A cross section (dashed line) of the contour map is displayed for each.

where θ is the angle between the electromagnetic wave k vector and the external magnetic field direction, and $\vec{\mu} \equiv (c/\omega)\vec{k}$. The dependence of the dispersion relation on the angle of propagation is a unique feature of the plasma, quite different from other media, which leads to anomalous diffraction. In our system, with the beam propagating in the \hat{z} direction, the obliquely propagating waves of the beam are those affected by the dispersion relation. Zhang *et al.* [5] showed that the effect can be described using equifrequency contour (EFC) plots of plasma. Thus, Fig. 1 shows an EFC plot for a frequency of 7.9 GHz, a magnetic field of 0.35 T, and electron densities of $n_e = 10^{12} \text{ cm}^{-3}$ and $n_e = 10^{11} \text{ cm}^{-3}$. In Fig. 1(a), the RHCP wave clearly displays a hyperbolic EFC. To understand the behavior in this case, v_g , the group velocity, must be examined. v_g gives the direction of energy flow for a plane wave and must be normal to the EFC on the intersection between the k vector and the EFC [11]. Thus, as shown by Smith *et al.* [2], such a slab will provide a degree of refocusing similar to a negative index material. In addition, this wave can only propagate through the plasma at limited angles, unlike the LHCP wave, which can propagate at almost all angles. To provide a qualitative understanding of anomalous beam propagation in plasma, numerical COMSOL simulations were conducted and are also presented in Fig. 1. In the simulation, a plane wave is launched through a slit into a plasma within a chamber. The chamber walls, which absorb most of the radiation but still reflect a portion of it, were simulated using a perfectly

matched layer boundary condition. As can be observed, for the case of a hyperbolic EFC, the beam seems to be guided in a similar manner to the results obtained in the case of Smith *et al.* [2], while for the low density plasma the beam diffracts similar to results obtained from the simulation for vacuum ($n_e = 0$).

In the series of experiments described below (a schematic of the experimental setup is presented in Fig. 2), a pulsed cold magnetized argon plasma is produced by a double folded Boswell-type [13] paddle-shaped antenna. This plasma is produced within a vacuum chamber, consisting of a 40 cm long glass tube of 17 cm diameter. On each side of the tube, metal flanges were fastened, each with a Plexiglas window and a series of ports. An arrangement of four axial solenoids is used to produce the necessary external magnetic field in the \hat{z} direction. In this arrangement, two pairs of coils of 18 cm diameter are placed symmetrically with respect to the chamber center. A 25 kJ capacitor bank drives the axial solenoids to produce an axial magnetic field of 0–4 T. The measurements have been performed at an axial magnetic field $B_0 = 0.4 \text{ T}$ corresponding to an electron cyclotron frequency of 11 GHz. The plasma electron density obtained during the period of interest is $n_e = 10^{12} \text{ cm}^{-3}$ corresponding to a plasma frequency of 9 GHz. The electron temperature of the plasma is $T_e < 0.7 \text{ eV}$, which has been measured by relative intensities and line broadening of the H_α and H_β spectral lines. This has also been used to confirm sufficient plasma uniformity. Tapered circularly polarized antennas are used for transmission and reception of microwaves and were selected due to relative polarization purity and large beam divergence. All experiments have been conducted below the cyclotron frequency with microwaves at a frequency of 7–8 GHz. The transmitting antenna and receiving antenna have been positioned internally, within the plasma chamber, to reduce interactions with the chamber windows or flanges that could mask the anomalous diffraction effect. The electron density is verified by transverse microwave cutoff-frequency measurements, which enables real-time density profile capture. Indeed, initial measurements in which transmitting and receiving RHCP antennas have been placed on opposite sides on the main axis of the plasma chamber have displayed a significant increase of the measured signal with plasma compared to the signal obtained for a non-ionized gas. As shown in Fig. 3, a 100 μs , 7.9 GHz pulse is transmitted through the plasma. This has been compared to an identical measurement, but without ionization of the gas. A substantial increase is observed in the received signal for plasma. This phenomenon of signal strengthening is obtained for varying magnetic field peak and for a span of frequencies between 7 and 8 GHz. To ensure that the plasma did not create interference in the antenna, a thin plastic cover has been used to seal the antenna aperture. The results remain unchanged. The effect of signal

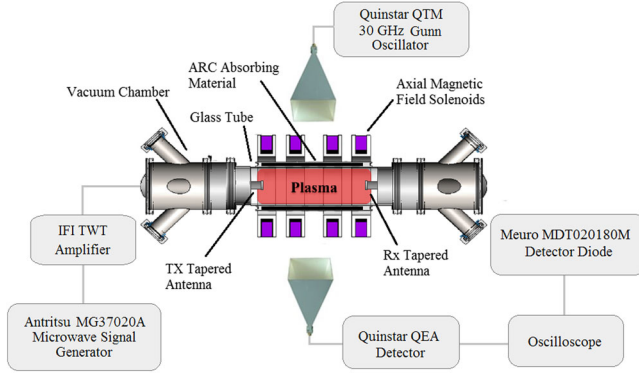


FIG. 2 (color online). Schematic of the experimental setup.

strengthening is evidence for the existence of anomalous diffraction in the plasma. Unlike self-focusing, in which the electromagnetic wave induces a change in the refractive index of the medium, in the case of anomalous diffraction the electromagnetic wave has little effect on the refractive index of the medium.

An interesting feature of the effect is observed for longer microwave pulses. As can be seen from Fig. 4 (blue, solid line), a 10 ms, 7.9 GHz pulse is initiated prior to ionization to measure the signal level in vacuum. Once the argon is ionized, at $t = 0$, the signal drops to zero. From this point, the magnetic field builds up and the electron density decreases. Only when the magnetic field is large enough, the plasma becomes transparent to the circularly polarized wave. The signal increase occurs almost immediately after the return from cutoff [region (2) in Fig. 4] for a brief time. Measurements of the plasma density at this time show that the density is approximately 10^{12} cm^{-3} . A question arises

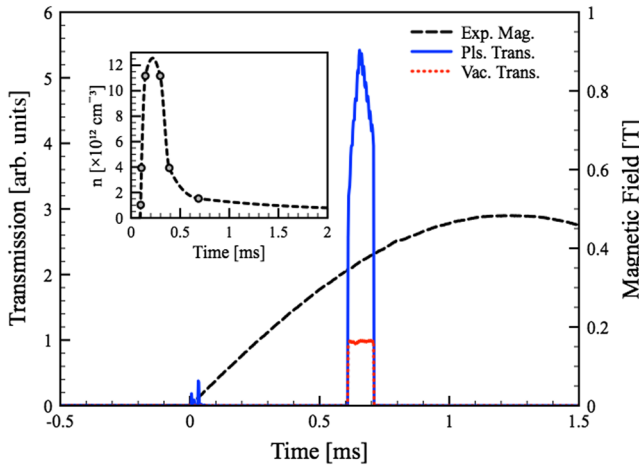


FIG. 3 (color online). Comparison of the measured signals for a $100 \mu\text{s}$, 7.9 GHz pulse, for the setup with plasma (blue, solid line) and without ionization (red, dotted line). Ionization begins at $t = 0$. A substantial increase can be observed in the measured signal in the case of plasma compared to nonionized gas. Inset: Measurement-based electron density profile.

as to why this effect is short lived. Bear in mind the constant decrease in the plasma density. For a density of 10^{12} cm^{-3} , $\omega_p > \omega$ and thus $\epsilon_p < 0$; in this case the plasma is a hyperbolic material. As previously mentioned, such a negative element in the permittivity tensor holds remarkable consequences for the electromagnetic properties of the material [11]. Soon after, the density decreases so that $\omega_p < \omega$, leading to $\epsilon_p > 0$, and the plasma is no longer hyperbolic for this frequency. The difference is illustrated in Fig. 1, where a comparison is presented between EFCs with electron densities of 1×10^{11} cm^{-3} ($\epsilon_p > 0$) and 1×10^{12} cm^{-3} ($\epsilon_p < 0$). It is clear that at electron densities of 1×10^{11} cm^{-3} the EFC dictates propagation very similar to vacuum. In fact, from these experimental measurements, we can clearly observe the transition of the plasma from a hyperbolic to a standard material for a given frequency. Thus, we understand that, unlike other metamaterials, for plasma there is an ability to control the influential parameters. To confirm these experimental results, the COMSOL model has been run quasistatically using the time-varying parameters of the experimental system. The electron density profile is assessed based on the discrete measurements that have been conducted. The signal at the detector is given by the Poynting vector amplitude at the

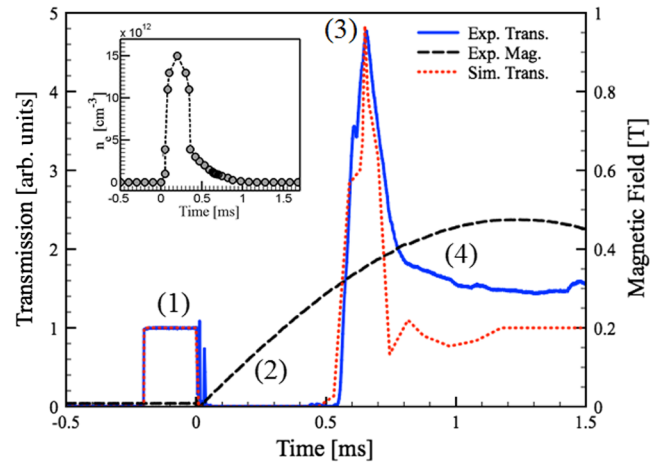


FIG. 4 (color online). Received signal of a 7.9 GHz, 10 ms pulse with the receiving antenna fixed on the main axis of the plasma chamber. Blue solid line, experimental results; red dotted line, simulation results. For comparison, the data were normalized to the experimental vacuum transmission level. Black dashed line, experimental magnetic field. (1) Transmission begins prior to ionization, to provide the vacuum signal for comparison. (2) At $t = 0$, ionization commences and the plasma becomes opaque, i.e., the cutoff region. The electron density for most of this period is above 1×10^{13} cm^{-3} . (3) Once the magnetic field builds up and the electron density decreases, transmission of the wave is possible. A signal increase is obtained immediately after cutoff. (4) The density decreases to a point that the effect no longer occurs and there is a return to previous transmission levels. Inset: Density profile used for the simulations.

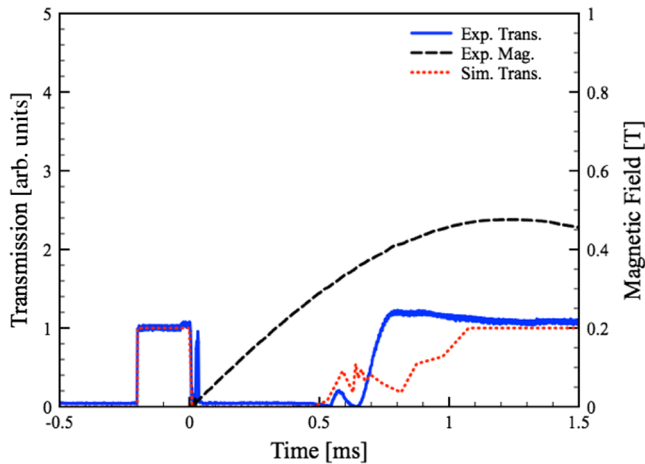


FIG. 5 (color online). Received signal of a 7.9 GHz, 10 ms pulse with the receiving antenna displaced 6 cm off the chamber main axis. Blue solid line, experimental results; red dotted line, simulation results. For comparison, the data were normalized to the experimental vacuum transmission level. Black dashed line, experimental magnetic field. Note that a significant signal increase is observed for the main axis results (Fig. 4) while the displaced results display no substantial signal increase.

experimental location of the detector in accordance with detector size. As can be observed from Fig. 4, for transmission of the same pulse as in the experiment, a very similar behavior is obtained. Indeed, with the simulation, it is possible to confirm that this effect occurs only for densities for which $\omega_p > \omega$. To examine the beam pattern during the period of the signal increase, the receiving antenna has been mounted at a radial distance of approximately 6 cm away from the main axis of the plasma chamber while the transmitting antenna is kept in the same position on the main axis of the plasma chamber. The results for a displaced receiving antenna and complementing simulation are presented in Fig. 5. There is a substantial difference between the two measurements depicted in Figs. 4 and 5. The on-axis measurement displays a significant signal increase, while the displaced antenna measurement presents no noticeable increase. From these results we can deduce that during the signal increase a larger fraction of the beam power is focused in the region of the main chamber axis. This greatly supports the anomalous diffraction interpretation. As can be observed from Fig. 5, the simulation results are consistent with the displaced antenna experimental results.

As previously mentioned, the signal strengthening is observed only at the densities predicted by the theoretical model and for a band of frequencies. This signal increase is not due to amplification of the intensity, but rather a result of a greater portion of the energy of the wave reaching the receiving antenna. Additional experiments confirmed a dependence between the level of signal increase and the transmission power, and we observed that the ratio between

the vacuum signal and the signal increase in the case of plasma is greater for antennas with greater beam divergence. Additional measurements that we have carried out confirm that the signal increase is not generated as a result of reflections, rotation of the polarization plane, improvement of antenna matching by the plasma, or density gradients within the plasma.

To summarize, this is the first time evidence has been provided for the existence of anomalous diffraction of electromagnetic waves in a cold magnetized plasma. Additionally, decreasing the electron density enables observation of the transition of the material from a hyperbolic to a standard material. Magnetized plasma, with appropriate control of the electron density and longitudinal magnetic field, can serve as a tunable hyperbolic medium. Moreover, the control parameters can be used to switch this medium between normal, dispersive behavior and anomalous, hyperbolic behavior. This enables the utilization of plasma in a similar context to reconfigurable metamaterials.

*Corresponding author.

zivabelson@hotmail.com

- [1] A. Poddubny, I. Iorsh, P. Belov, and Y. Kivshar, Hyperbolic metamaterials, *Nat. Photonics* **7**, 948 (2013).
- [2] D. R. Smith, D. Schurig, J. J. Mock, P. Kolinko, and P. Rye, Partial focusing of radiation by a slab of indefinite media, *Appl. Phys. Lett.* **84**, 2244 (2004).
- [3] Z. Liu, H. Lee, Y. Xiong, C. Sun, and X. Zhang, Far-field optical hyperlens magnifying sub-diffraction-limited objects, *Science* **315**, 1686 (2007).
- [4] Z. Jacob, I. I. Smolyaninov, and E. E. Narimanov, Broadband Purcell effect: Radiative decay engineering with metamaterials, *Appl. Phys. Lett.* **100**, 181105 (2012).
- [5] S. Zhang, Y. Xiong, G. Bartal, X. Yin, and X. Zhang, Magnetized Plasma for Reconfigurable Subdiffraction Imaging, *Phys. Rev. Lett.* **106**, 243901 (2011).
- [6] R. K. Fisher and R. W. Gould, Resonance Cones in the Field Pattern of a Short Antenna in an Anisotropic Plasma, *Phys. Rev. Lett.* **22**, 1093 (1969).
- [7] R. Gad, J. G. Leopold, A. Fisher, D. R. Fredkin, and A. Ron, Observation of Magnetically Induced Transparency in a Classical Magnetized Plasma, *Phys. Rev. Lett.* **108**, 155003 (2012).
- [8] F. F. Chen, *Introduction to Plasma Physics and Controlled Fusion* (Springer, New York, 1984).
- [9] J. B. Pendry, Negative Refraction Makes a Perfect Lens, *Phys. Rev. Lett.* **85**, 3966 (2000).
- [10] J. B. Pendry, *Photonic Crystals and Light Localization in the 21st Century* (Springer, New York, 2001), pp. 329–349.
- [11] D. R. Smith and D. Schurig, Electromagnetic Wave Propagation in Media with Indefinite Permittivity and Permeability Tensors, *Phys. Rev. Lett.* **90**, 077405 (2003).
- [12] M. A. Heald and C. B. Wharton, *Plasma Diagnostics with Microwaves* (R. E. Krieger, Huntington, 1978).
- [13] R. W. Boswell, Plasma production using a standing helicon wave, *Phys. Lett.* **33A**, 457 (1970).